Cell Tissue Res (2017) 370:99–112
DOI 10.1007/s00441-017-2646-4

REGULAR ARTICLE

Cell type-specific localization of Ephs pairing with ephrin-B2 in the rat postnatal pituitary gland

Saishu Yoshida[1,2] · Takako Kato[2] · Naoko Kanno[1] · Naoto Nishimura[1] · Hiroto Nishihara[1] · Kotaro Horiguchi[3] · Yukio Kato[1,2,4]

Received: 3 October 2016 / Accepted: 6 May 2017 / Published online: 28 June 2017

Abstract *Sox2*-expressing stem/progenitor cells in the anterior lobe of the pituitary gland form two types of micro-environments (niches): the marginal cell layer and dense cell clusters in the parenchyma. In relation to the mechanism of regulation of niches, juxtacrine signaling via ephrin and its receptor Eph is known to play important roles in various niches. The ephrin and Eph families are divided into two subclasses to create ephrin/Eph signaling in co-operation with confined partners. Recently, we reported that ephrin-B2 localizes specifically to both pituitary niches. However, the Ephs interacting with ephrin-B2 in these pituitary niches have not yet been identified. Therefore, the present study aims to identify the Ephs interacting with ephrin-B2 and the cells that produce them in the rat pituitary gland. In situ hybridization and immunohistochemistry demonstrated cell type-specific localization of candidate interacting partners for ephrin-B2, including EphA4 in cells located in the posterior lobe, EphB1 in gonadotropes, EphB2 in corticotropes, EphB3 in stem/progenitor cells and EphB4 in endothelial cells in the adult pituitary gland. In particular, double-immunohistochemistry showed *cis*-interactions between EphB3 and ephrin-B2 in the apical cell membranes of stem/progenitor cell niches throughout life and *trans*-interactions between EphB2 produced by corticotropes and ephrin-B2 located in the basolateral cell membranes of stem/progenitor cells in the early postnatal pituitary gland. These data indicate that ephrin-B2 plays a role in pituitary stem/progenitor cell niches by selective interaction with EphB3 in *cis* and EphB2 in *trans*.

Keywords Rat pituitary · Stem/progenitor cells · Niche · Ephrin-B2 · EphB3

Abbreviations

CAR	Coxsackievirus and adenovirus receptor
DAPI	4,6-Diamidino-2-phenylindole
Eph	Erythropoietin-producing hepatocellular carcinoma receptor
Ephrin	Eph family receptor interacting proteins
FITC	Fluorescein isothiocyanate
MCL	Marginal cell layer
PCR	Polymerase chain reaction
PDZ	PSD-95, Dlg, ZO-1
PFA	Paraformaldehyde
SOX2	Sex-determining region Y-box 2
SVZ	Subventricular zone
TBP	TATA-box-binding protein

Introduction

The pituitary gland is a master endocrine tissue composed of two anatomically different entities: the adenohypophysis (anterior pituitary), composed of the anterior and intermediate lobes and the neurohypophysis of the posterior lobe. The anterior lobe of the pituitary gland has five endocrine cell-types, including somatotropes, which produce growth hormone (GH); lactotropes, which produce prolactin (PRL); thyrotropes, which

✉ Yukio Kato
yukato@meiji.ac.jp

[1] Division of Life Science, Graduate School of Agriculture, Meiji University, Kanagawa, Japan

[2] Institute of Reproduction and Endocrinology, Meiji University, Kanagawa, Japan

[3] Laboratory of Anatomy and Cell Biology, Department of Health Sciences, Kyorin University, Tokyo, Japan

[4] Department of Life Science, School of Agriculture, Meiji University, Kanagawa, Japan

produce thyroid-stimulating hormone (TSH); gonadotropes, which produce follicle-stimulating hormone (FSH) and luteinizing hormone (LH); and corticotropes, which produce adrenocorticotropic hormone (ACTH). During rodent pituitary development, corticotropes first appear in the ventral part of the anterior lobe. Subsequently, PIT1-commitment cells (origin of somatotropes, lactotropes and thyrotropes) and gonadotropes start to differentiate in the caudomedial region and the most ventral part of the anterior lobe, respectively (Zhu et al. 2007). Afterward, those five types of endocrine-cells are scattered in the parenchyma of the anterior lobe. The cellular composition of each endocrine cell is regulated by a number of transcription factors and growth factors during not only embryonic organogenesis but also a postnatal growth wave in the first-to-third weeks after birth, when proliferation and differentiation actively occur in the anterior lobe (Davis et al. 2010; Vankelecom and Chen 2014; Ward et al. 2005; Zhu et al. 2007). In addition, stem/progenitor cells exist as non-endocrine cells and play roles in the regeneration of the adult pituitary gland (Fu et al. 2012; Fu and Vankelecom 2012; Vankelecom and Chen 2014; Willems et al. 2016). Among these cells, recent studies have demonstrated that *Sox2*-expressing cells are important in the physiological maintenance of the adult pituitary gland through an in vitro assay using pituispheres (Chen et al. 2009; Fauquier et al. 2008) and an in vivo assay using $Sox2^{CreERT2/+}$; $R26^{YFP/+}$ transgenic mice (Andoniadou et al. 2013; Chen et al. 2009; Fauquier et al. 2008; Fu et al. 2012; Fu and Vankelecom 2012; Rizzoti et al. 2013).

A niche is a microenvironment containing stem cells and niche cells that maintain stemness through paracrine and juxtacrine factors. Niches have been identified in tissues such as the brain, intestine and skin (Chen and Chuong 2012). In the adult pituitary gland, marginal cell layer (MCL-niche) and SOX2-positive cell clusters scattering in the parenchyma of the anterior lobe (parenchymal-niche) are postulated as niches (Gremeaux et al. 2012; Vankelecom and Chen 2014; Yoshida et al. 2016a). While the MCL-niche persists throughout early embryonic and adult development of the anterior pituitary gland, the parenchymal-niche only appears after birth, increasing in number during the early postnatal pituitary growth wave (Chen et al. 2013). Recently, we demonstrated the existence of two transmembrane proteins that are present in both pituitary niches: the transmembrane protein CAR (coxsackievirus and adenovirus receptor), which is encoded by the *Cxadr* gene and is able to form homophilic tight junctions (Chen et al. 2013); and the juxtacrine factor ephrin-B2 (Yoshida et al. 2015). More recently, we isolated the parenchymal-niche by taking advantage of its tight structure and resistance to protease treatment (Yoshida et al. 2016b). These data suggest that cell-to-cell communication is important for the construction and regulation of pituitary gland niches. However, the functions of these membrane proteins in the maintenance of stem/progenitor cells and *trans*-differentiation in the pituitary niche remain unclear.

Ephrin and its receptor Eph are signaling molecules that localize to cell membranes and turn on juxtacrine signaling through cell-to-cell adhesion (Arvanitis and Davy 2008). Ephrin/Eph signaling is known to play important roles in various niches, such as the subventricular zone (SVZ) in the brain (Nomura et al. 2010), the crypts of the intestine (Batlle et al. 2002) and the hair follicles of the skin (Genander et al. 2010). Two types of interactions are known to occur between ephrin and Eph (see the schema about the interaction of ephrin and Eph in Arvanitis and Davy 2008; Kania and Klein 2016). The first is a *trans*-interaction where each of *ephrin* and *Eph* is expressed in opposing cells; this activates bi-directional signaling in both the *Eph*-expressing cell (termed forward signaling) and the *ephrin*-expressing cell (reverse signaling). The second is a *cis*-interaction, in which both molecules are co-expressed in the same cell, generating inactive (parallel or anti-parallel) signaling (Arvanitis and Davy 2008; Egea and Klein 2007; Kania and Klein 2016). The ephrin and Eph families

Table 1 List of primer sets of quantitative real-time PCR

Gene	Sequence (5'→3')		Production size (bp)	Accession no.
EphA4	Forward	TGGGCTGAGACAATCCTGA	160	NM_001162411.1
	Reverse	AGGAACCAAGGAGGGTGTG		
EphB1	Forward	TACCACCGTGGATGACTGG	240	NM_001104528.1
	Reverse	TCCTCCCCTAGGAACATCG		
EphB2	Forward	GTCTGACTTCGGGCTCTCAC	134	NM_001127319.1
	Reverse	TGGCTGAGGTGAATTTCCGG		
EphB3	Forward	AAGGATCGGGGTCACTTTG	158	NM_001105868.1
	Reverse	GGGGATATCACCCCCTCTT		
EphB4	Forward	GCTCCTTTGAGGTGGTCAGCCA	126	XM_003751157.4
	Reverse	CTCCTGGCTTAGCTTGGGAC		
EphB6	Forward	TTCCTTGCCTGGACTCTCC	192	NM_001107857.1
	Reverse	GCTGGAGGAGCTGGATGTT		
Tbp	Forward	GATCAAACCCAGAATTGTTCTCC	134	NM_001004198.1
	Reverse	ATGTGGTCTTCCTGAATCCC		

Table 2 List of primary antibodies

Section type	Antigen-retrieval	Antibody description	Vendor	Target cell/molecule	Dilution	References for validation of antibodies
95% ethyl alcohol fixed-cryosection	-	Mouse monoclonal IgG against human ephrin-B2 (clone EFR-163 M)	[1]	Pituitary stem/progenitor cell	1:150	Yoshida et al. 2015
		Goat IgG against mouse EphB3	[2]	*	1:100	Batlle et al. 2002
		Goat IgG against human EphB4	[2]	*	1:400	Ishii et al. 2011
		Mouse monoclonal IgG against rat PECAM	[3]	Endothelial cell	1:30	Zaglia et al. 2016
	-	Alexa Flour 488 congugated Phalloidin	[4]	F-action	1:100	Wollesen et al. 2009
		Mouse monoclonal IgG against human EphB1	[5]	*	1:1.000	Anselmo et al. 2016
	$80^{¨}C^{+}$, 1 h	Goat IgG against human EphB2	[2]	*	1:400	Batlle et al. 2002
		Mouse IgG against human E-cadherin	[3]	Pituitary stem/progenitor cell	1:250	Kikuchi et al. 2007
		FITC congugated Isoleetin-B4	[6]	Endothelial cell	1:100	Higuchi et al. 2015
		Guinea pig antiserum against rat FSHβ	[7]	Gonadotropes	1:100,00	[7]
		Guinea pig antiserum against ovine LHβ		Gonadotropes	1:20,000	
		Guinea pig antiserum against rat PRL		Lactotropes	1:70,000	
		Guinea pig antiserum against rat TSHβ		Thyrotropes	1:100,000	
		Guinea pig antiserum against human ACTH	[8]	Conticotropes	1:50,000	Tanaka and Kurosumi 1992
		Guinea pig antiserum against human GT		Somatotrops	1:50,000	Kato et al. 2004
	$120^{¨}C^{+}$, 5 min	Mouse monoclonal IgG against human ephrin-B2 (clone EFR-163 M)	[1]	Pituitary stem/progenitor cell	1:50	Yoshida et al. 2015
		Goat IgG against human EphB2	[2]	*	1:400	Batlle et al. 2002

*indicates "Tested in this study"

+ and – indicate with or without antigen-retrieval using ImmunoSaver (0.05% citraconic anhydride solution, pH 7.4), respectively.

[1] SIGMA, St. Louis, MO, USA, [2] R&D Systems, Minneapolism MN, USA, [3] BD Biosciences, San Jose, CA, USA, [4] Thermo Scientific, Waltham, MA, USA, [5] Abcam, Cambridge, UK, [6] Vector, Burlingame, CA, USA, [7] kindly provided by the National Institute of Diabetes and Digestive and Kindy Disease (NIDDK) through the courtesy of Dr. A.F. Parlow, [8] kindly provided by Dr. S. Tanaka at Shizuoka University, Shizuoka, Japan

are divided into two subclasses, with five ephrin-A, three ephrin-B, nine EphA and five EphB proteins (Murai and Pasquale 2003; Pasquale 2005). Among these, B-class ephrin/Eph signaling is responsible for intercellular signaling between stem cells and neighboring cells (e.g., niche cells and differentiated cells) in various tissues such as the crypt (Batlle et al. 2002), subgranular zone, (Ashton et al. 2012) and SVZ (Nomura et al. 2010). As described above, we reported that ephrin-B2 exists in SOX2/CAR-double positive stem/progenitor cells in both the MCL- and parenchymal-niches in the pituitary gland, suggesting that ephrin-B2 is a molecular regulator of pituitary stem/progenitor cell niches (Yoshida et al. 2015). Although ephrin-B2 has a potential to interact with EphA4, EphB1, EphB2, EphB3, EphB4 and EphB6, the interacting partner Ephs for ephrin-B2 in the adult pituitary stem/progenitor cell niches have not yet been identified.

In this study, we aim to identify the Ephs pairing with ephrin-B2 and the cells that produce them in the postnatal rat pituitary gland. Immunohistochemistry of candidate Ephs pairing with ephrin-B2 demonstrated that ephrin-B2 and EphB3 exist in the same cell membrane, suggesting a *cis*-interaction in adult pituitary stem/progenitor cell niches. In contrast, during the postnatal growth wave, we found a transition in the membrane localization of ephrin-B2, resulting in the formation of a *trans*-interaction with EphB2 produced by corticotropes. These data suggest that ephrin-B2 regulates pituitary stem/progenitor cell niches through selective interaction with EphB3 in *cis* and EphB2 in *trans*.

Materials and methods

Animals

Intact Wistar-Imamichi strain rats (0–9 weeks) were housed individually in a temperature-controlled room under a 12-h light/12-h dark cycle. Determination of pregnancy was made by the observation of a vaginal plug on day 0.5 of gestation. Rats were killed by cervical dislocation under anesthesia. The present study was approved by the Institutional Animal Care and Use Committee, Meiji University and complied with the NIH Guidelines for the Care and Use of Laboratory Animals.

Quantitative real-time polymerase chain reaction (PCR)

Total RNAs were extracted from each of the anterior and intermediate/posterior lobe of postnatal day 60 (P60, $n = 3$) rats using ISOGEN (Nippon Gene, Tokyo, Japan). Reverse transcripts were synthesized with PrimeScript Reverse Transcriptase (Takara Bio, Otsu, Japan) using 1 μg of total RNAs after DNase I treatment and were subjected to quantitative real-time PCR on the ABI Prism 7500 Real-Time PCR System (Applied Biosystems, Foster City, CA, USA). Reactions were performed in SYBR Green Real-Time PCR Master Mix Plus (Toyobo, Osaka, Japan) and included 0.6 μM of a specific primer set for each gene (Table 1). Each sample was measured in two independent experiments and data were quantified using the comparative C_T method (DC_T method) to estimate the gene copy number relative to *Tbp* as an internal standard. The DNA sequence of the PCR product from each sample was confirmed by nucleotide sequencing (data not shown).

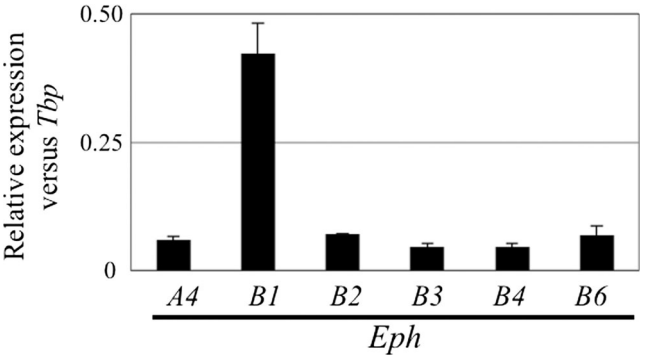

Fig. 1 Expression of candidate Ephs interacting with ephrin-B2 in the anterior lobe of the adult pituitary gland. Quantitative real-time polymerase chain reaction (PCR) was performed to estimate mRNA levels of candidate binding partners *EphA4*, *EphB1*, *EphB2*, *EphB3*, *EphB4* and *EphB6* using total RNAs prepared from the anterior lobe on P60. Data were calculated using the comparative C_T method to estimate copy number relative to that of the TATA box binding protein gene (*Tbp*), which was used as an internal standard. Data are presented as means ± SD in two independent experiments

Fig. 2 Localization of EphA4, EphB1, EphB2 and EphB4 in the adult pituitary gland. **a**–**a‴** In situ hybridization of *EphA4* using 4% PFA-fixed frozen sections of the pituitary gland on P60. A positive signal for the anti-sense probe was detected in the posterior lobe (*boxed area* in **a′** is enlarged in **a″**) and no signal was detected by the sense probe in the posterior lobe (**a‴**). **b** Expression of *EphA4* in each of the adult anterior and intermediate/posterior lobe (P60) as determined by real-time PCR. Data were quantified and are presented as described in Fig. 1. **c**–**d⁗** Double-immunohistochemistry for EphB1 and LHβ using 4% PFA-fixed frozen sections of the pituitary gland on P60. Merged image of EphB1 visualized with Cy3 (*red*) and nuclear staining by 4,6-Diamidino-2-phenylindole (DAPI, *blue*) is shown in (**c**). The *boxed area* in (**d**) is enlarged in **d′** (EphB1), **d″** (LHβ with Cy5; *green*), **d‴** (merge) and **d⁗** (merge with DAPI). **e**–**f⁗** Double-immunohistochemistry for EphB2 and ACTH using 4% PFA-fixed frozen sections of the pituitary gland on P60. Merged image of EphB2 visualized with Cy3 (*red*) and nuclear staining by DAPI (*blue*) is shown in (**e**). The *boxed area* in (**f**) is enlarged in **f′** (EphB2) and **f″** (ACTH with Cy5; *green*), **f‴** (merge) and **f⁗** (merge with DAPI). **g**–**h⁗** Double-immunohistochemistry for EphB4 and PECAM using 95% ethyl alcohol-fixed cryosections of the pituitary gland on P60. Merged image of EphB4 visualized with Cy3 (*red*) and nuclear staining by DAPI (*blue*) is shown in (**g**). The *boxed area* in (**h**) is enlarged in **h′** (EphB4) and **h″** (PECAM with Cy5; *green*), **h‴** (merge) and **h⁗** (merge with DAPI). *Dotted lines* in **a**, **c**, **e** and **g** outline the anterior, intermediate and posterior lobes. *Arrowheads* and *arrows* in **h′**–**h⁗** indicate EphB4/PECAM-double positive cells and EphB4-single positive cells adjacent to PECAM-single positive cells, respectively. All images were observed using a BZ-8000 epifluorescence microscope. *AL* anterior lobe; *IL* intermediate lobe; *PL* posterior lobe. *Bars* (**a**, **c**, **e**, **g**) 50 μm, (**a″**, **a‴**, **d⁗**, **f⁗**, **h⁗**) 20 μm

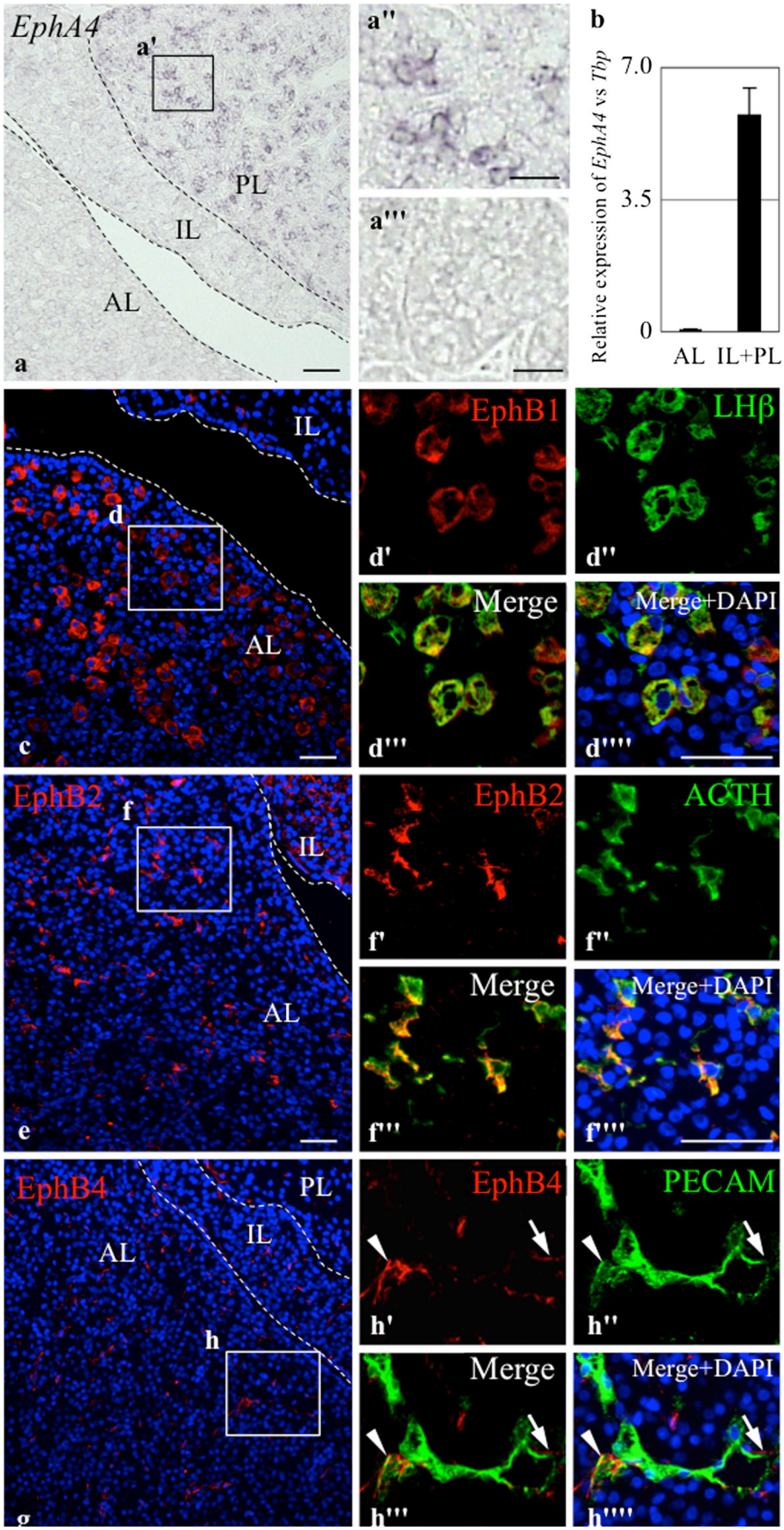
EphA4
a'
PL
IL
AL
a
a''
a'''
b
Relative expression of EphA4 vs Tbp
7.0
3.5
0
AL IL+PL
IL
d
AL
c
EphB1
d'
LHβ
d''
Merge
d'''
Merge+DAPI
d''''
EphB2
f
IL
AL
e
EphB2
f'
ACTH
f''
Merge
f'''
Merge+DAPI
f''''
EphB4
PL
IL
AL
h
g
EphB4
h'
PECAM
h''
Merge
h'''
Merge+DAPI
h''''

Immunohistochemistry

Immunohistochemistry was performed after fixation with 95% ethyl alcohol or 4% paraformaldehyde (PFA). The method of fixation was selected according to the antibody used (Table 2). Fixation and immunostaining were performed as follows. For ethyl alcohol fixation, freshly prepared pituitaries of embryonic day (E) 11.5, E12.5, E13.5, E16.5, E20.5, P5 and P60 rats were embedded in Tissue-Tek O.C.T. compound (Sakura Finetek Japan, Tokyo, Japan) and frozen immediately. Cryosections (7 μm thick) from the sagittal planes of embryonic pituitaries and coronal planes of postnatal pituitaries were mounted on glass slides (Matsunami, Osaka, Japan), followed by fixation in 95% ethyl alcohol for 30 min at −20 °C. For PFA fixation, the pituitaries of E13.5, P5 and P60 rats were fixed with 4% PFA in 20 mM HEPES (pH 7.5) overnight at 4 °C, followed by immersion in 30% trehalose in 20 mM HEPES to cryoprotect the tissues. They were embedded in Tissue-Tek O.C.T. compound and frozen immediately. Frozen sections (7 μm thick) from the sagittal planes of embryonic pituitaries and coronal planes of postnatal pituitaries were prepared. Depending on the antibody, sections were antigen-retrieved by an ImmunoSaver (0.05% citraconic anhydride solution, pH 7.4; Nisshin EM, Tokyo, Japan) (Table 1).

After washing with 20 mM HEPES and 100 mM NaCl (pH 7.5; HEPES buffer), the sections were reacted with primary antibodies at appropriate dilutions (Table 1) with 10% (v/v) fetal bovine serum (FBS) or 0.5% bovine serum albumin (BSA) in HEPES buffer (blocking buffer) overnight at 4 °C. After the immunoreaction, the sections were washed with HEPES buffer and then incubated with secondary antibodies using Cy3-, Cy5-, or FITC-conjugated AffiniPure donkey anti-mouse, rabbit, goat and guinea pig IgG (1:500 dilution; Jackson ImmunoResearch, West Grove, PE, USA). The sections were washed with HEPES buffer and then enclosed in VECTASHIELD Mounting Medium with 4′, 6-diamidino-2-phenylindole (DAPI) (Vector, Burlingame, CA, USA). Immunofluorescence was observed under a BZ-8000 fluorescence microscope (KEYENCE, Osaka, Japan) or a FLUOVIEW FV1000 confocal microscope (Olympus, Tokyo, Japan). The number of cells neighboring the MCL-zone and parenchymal-niches of the anterior lobe were measured by counting six MCL sections (1.9 ± 0.19 mm each) and nine parenchymal areas (0.2 mm^2 each) in the sections prepared from three P5 rats. In the parenchyma, dense cell clusters composed of more than four SOX2-positive cells (assumed based on E-cadherin) were regarded as belonging to the parenchymal-niche (Yoshida et al. 2016b). Data are presented as means ± SD.

In situ hybridization

In situ hybridization was performed with digoxigenin (DIG)-labeled cRNA probes according to a previous method (Fujiwara et al. 2008). Briefly, the 5′ region of the coding sequence for rat *EphA4* (1–812 bp) was ligated to pBluescript SK+ (Stratagene, La Jolla, CA, USA) and DIG-labeled cRNA probes were prepared using Roche DIG RNA labeling kit (Roche Diagnostics, Penzberg, Germany). Next, 4% PFA-fixed frozen sections of the coronal plane (5 μm thick) were hybridized with DIG-labeled cRNA probe at 57 °C for 16 h. After hybridization, sections were incubated with alkaline phosphatase-conjugated anti-DIG antibody (1:1000 dilution; Roche Diagnositcs) for 1 h at room temperature and were visualized with 4-nitroblue tetrazolium chloride (NBT; Roche Diagnostics) and 5-bromo-4-chloro-3-indolyl phosphate (BCIP; Roche Diagnostics). Microscopic observation was performed with the BZ-8000. A control experiment was performed with the DIG-labeled sense cRNA probe.

Results

Gene expression and cell type-specific localization of candidate Ephs interacting with ephrin-B2 in the adult pituitary gland

We recently reported that *ephrin-B2*, which has a potential to interact with EphA4, EphB1, EphB2, EphB3, EphB4 and EphB6, is expressed in the pituitary stem/progenitor cell niches of the adult anterior lobe (Yoshida et al. 2015). Therefore, we examined the expression in these niches of candidate Ephs interacting with ephrin-B2 (*EphA4*, *EphB1*, *EphB2*, *EphB3*, *EphB4* and *EphB6*) (Jensen 2000; Munthe et al. 2000) by quantitative real-time PCR analysis. The results demonstrated that all candidate Ephs were expressed in the anterior lobe (Fig. 1). In particular, *EphB1* was the most highly expressed among the Ephs examined.

Next, we sought to determine the cellular localizations of Ephs interacting with ephrin-B2. Among them, localization analysis was not conducted for EphB6 because EphB6 is a kinase-dead Eph (Gurniak and Berg 1996) and shows a complicated property to interact not only with EphB1 (Freywald et al. 2002) and EphB4 (Truitt et al. 2010) but also with another A-class Eph, EphA2 (Akada et al. 2014). Therefore, we focused on typical Ephs (EphA4, EphB1, EphB2, EphB3 and EphB4) as binding partners for ephrin-B2. As an appropriate antibody against EphA4 was lacking, we performed in situ hybridization for *EphA4*. Immunohistochemistry was used for localization of EphB1, EphB2, EphB3 and EphB4. In situ hybridization demonstrated that *EphA4* was strongly expressed by nucleated cells in the adult posterior lobe but not in the anterior and intermediate lobes (Fig. 2a–a‴). Real-time PCR also confirmed that *EphA4* was expressed at much higher levels in the intermediate/posterior lobe than in the anterior lobe (Fig. 2b).

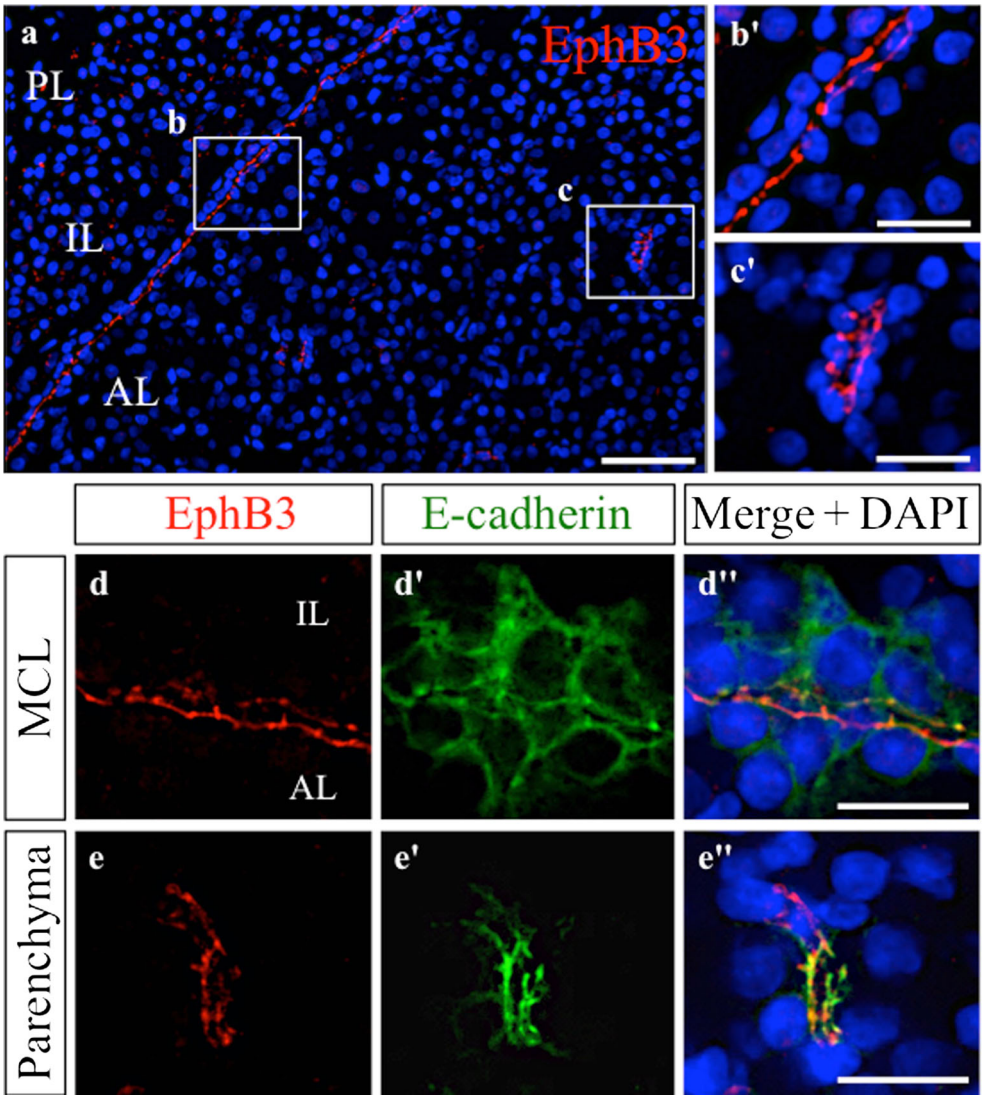

Fig. 3 Localization of EphB3 in the adult pituitary stem/progenitor cell niches. **a**–**c′** Immunohistochemistry for EphB3 using 95% ethyl alcohol-fixed cryosections of the pituitary gland on P60. Merged image with EphB3 visualized with Cy3 (*red*) and nuclear staining by DAPI (*blue*) is shown in (**a**) and the *boxed areas* in (**b** and **c**) are enlarged in (**b′** and **c′**), respectively. **d**–**e″** Double-immunohistochemistry for EphB3 and stem/progenitor cell marker E-cadherin using 95% ethyl alcohol-fixed cryosections of the pituitary gland on P60. EphB3 visualized with Cy3 (*red*) (**d**, **e**), E-cadherin visualized with Cy5 (*green*) (**d′**, **e′**) and merged images with nuclear staining by DAPI (*blue*) (**d″**, **e″**) in the MCL (**d**–**d″**) and the parenchyma of the anterior lobe (**e**–**e″**) are shown. All images were observed using a BZ-8000 epifluorescence microscope. *AL* anterior lobe; *IL* intermediate lobe; *MCL* marginal cell layer; *PL* posterior lobe. *Bars* (**a**) 50 μm, (**b′**, **c′**, **d″**, **e″**) 20 μm

Immunohistochemistry for EphB1, EphB2 and EphB4 showed that all three were present in the adult anterior lobe (Fig. 2c–g). Double-immunohistochemistry demonstrated that EphB1 and EphB2 were specifically located in terminally differentiated cells, with expression in LHβ-positive gonadotropes (Fig. 2c–d′′′′) and ACTH-positive corticotropes (Fig. 2e–f′′′′), respectively. Notably, both EphB1 and EphB2 localized to the cytoplasm (Fig. 2d′, f′) whereas we could not confirm whether EphB1 and EphB2 localized to cell-surface membranes in the adult pituitary. Next, double-immunohistochemistry for EphB4 and the vascular endothelial cell marker PECAM demonstrated some EphB4 signals located in PECAM-positive endothelial cells (Fig. 2h′-h′′′′, arrowheads) and contiguous cells (Fig. 2h′-h′′′′, arrows). These same *EphA4,* EphB1, EphB2 and EphB4 localization patterns were observed in the neonatal pituitary gland on P5 (data not shown).

In contrast, immunohistochemistry for EphB3 demonstrated that EphB3 was present in the cell-surface membranes of cells located on both the anterior and intermediate sides of the MCL, as well as in cell clusters scattered throughout the parenchyma of the anterior lobe (Fig. 3a–c′). Double-immunohistochemistry for EphB3 and E-cadherin, which is a pituitary stem/progenitor cell marker (Fauquier et al. 2008), demonstrated that EphB3 co-localized with E-cadherin in both

Table 3 Summary of localization of Ephs paring with ephrin-B2

Factor	Localization
EphA4	Nucleated cells in the posterior lobe
EphB1	Gonadotropes
EphB2	Corticotropes
EphB3	Pituitary stem/progenitor cell niche
EphB4	Endothelial cells and contiguous cells involved in the vasculature

the MCL- and parenchymal-niche of the anterior lobe (Fig. 3d–e″).

In summary, candidate Ephs interacting with ephrin-B2 exhibited cell type-specific localization in the pituitary gland, with *EphA4* present in cells in the posterior lobe, EphB1 in gonadotropes, EphB2 in corticotropes, EphB4 in endothelial cells and contiguous cells involved in the vasculature and EphB3 in both pituitary stem/progenitor cell niches (Table 3).

Localization of EphB3 during pituitary development

As EphB3 exhibited a similar localization pattern to that of ephrin-B2 in adult pituitary stem/progenitor cell niches (described in Yoshida et al. 2015), EphB3 represented a likely interacting partner for ephrin-B2. First, to confirm localization of EphB3 in the MCL-niche during embryonic pituitary development (before the parenchymal niche has formed), we performed immunohistochemistry for EphB3 from E11.5 to E20.5 (Fig. 4). On E11.5 and E12.5, during the early stage of pituitary development, immunohistochemistry demonstrated that EphB3 signals existed in the cell membrane of the ventral region of the invaginating oral epithelium (Fig. 4a, b). On E13.5, when the invaginating oral epithelium forms the pituitary primordium of Rathke's pouch, EphB3 signals in the MCL localized specifically to the cell membranes facing the lumen (Fig. 4c) and this localization pattern was maintained on E16.5 (Fig. 4d) and E20.5 (Fig. 4e).

Localization of EphB3 and ephrin-B2 in the adult pituitary stem/progenitor cell niches

Next, we performed double-immunohistochemistry to confirm co-localization of EphB3 and ephrin-B2 in the postnatal pituitary stem/progenitor cell niches (Figs. 5 and 6). On P60, most of the EphB3 and ephrin-B2 signals co-localized to the restricted cell surface in both the MCL-niche (Fig. 5a–a″) and the parenchymal-niche of the anterior lobe (Fig. 5b–b″). Since we have reported that most of ephrin-B2 co-localize with S100β (Yoshida et al. 2015), EphB3-positive cells were presumed to be positive for S100β (data not shown). We further analyzed the polarity of the cells composing both niches by double-staining for SOX2 and phalloidin, which specifically binds to filamentous actin (F-actin) to delineate the apical cell surface of polarized cells (Li et al. 2007). The results demonstrated that the cells in a single layer of both niches were highly polarized, with the apical surface of cells in the MCL-niche facing the residual lumen (Fig. 5c–c″) and that of cells in the parenchymal-niche facing the central lumen (Fig. 5d–d″). The localization patterns of EphB3 and ephrin-B2 in both niches (Fig. 5a–b″) coincided with that of phalloidin, demonstrating that both EphB3 and ephrin-B2 are limited to the apical cell membrane of the polarized cells in the two niches.

Next, we examined the localization of EphB3 and ephrin-B2 in the neonatal pituitary gland on P5, when the postnatal pituitary growth wave is initiated (Davis et al. 2010; Vankelecom and Chen 2014; Ward et al. 2006; Zhu et al. 2007), followed by formation of the MCL-zone beneath the MCL and the parenchymal-niche (Chen et al. 2013). The results demonstrated that, although the

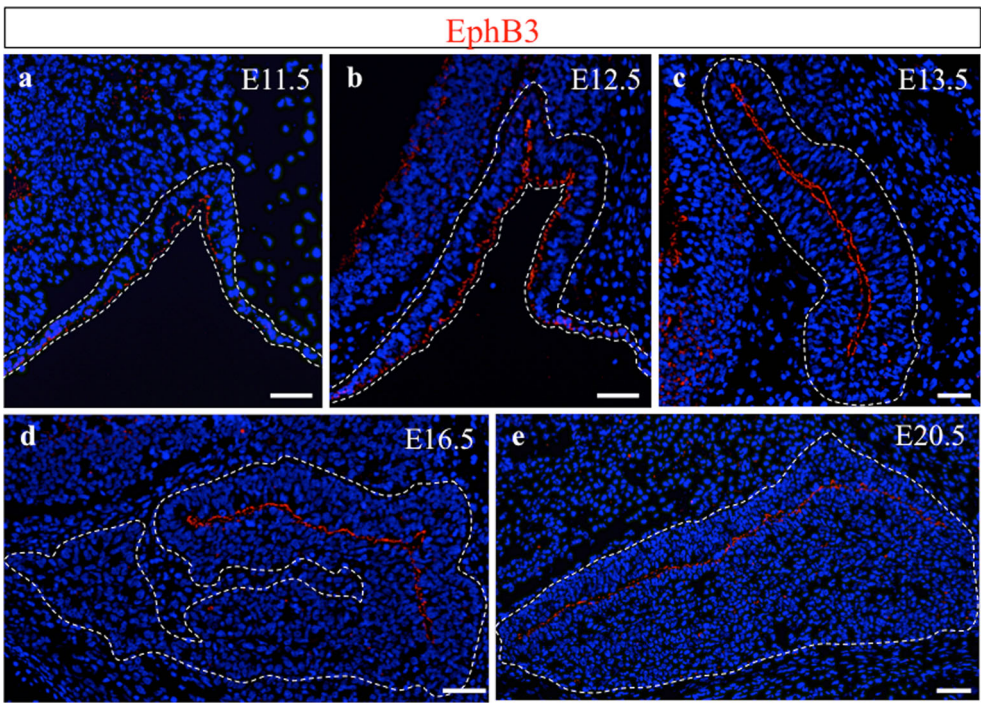

Fig. 4 Localization of EphB3 during pituitary development. Immunohistochemistry for EphB3 using 95% ethyl alcohol-fixed cryosections of the pituitary gland on E11.5 (**a**), E12.5 (**b**), E13.5 (**c**), E16.5 (**d**) and E20.5 (**e**). Merged images with EphB3 visualized with Cy3 (*red*) and nuclear staining by DAPI (*blue*) are shown in (**a**–**e**). *Dotted lines* outline the anterior and intermediate lobes. All images were observed using a BZ-8000 epifluorescence microscope. *Bars* 50 μm

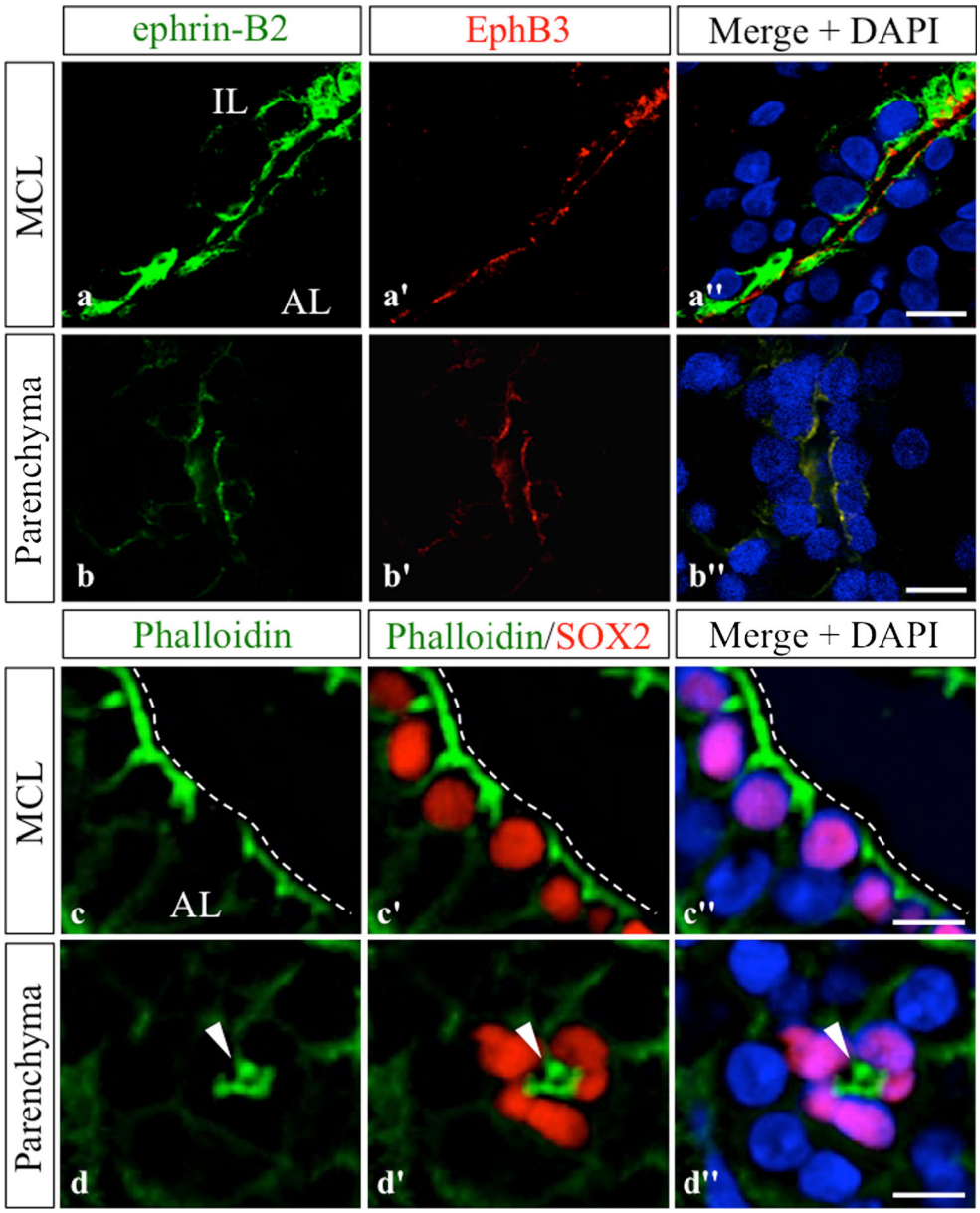

Fig. 5 Co-localization of ephrin-B2 and EphB3 in both niches in the adult pituitary gland. Immunohistochemistry for ephrin-B2 and EphB3 was performed using 95% ethyl alcohol-fixed cryosections of the pituitary gland on P60. Ephrin-B2 visualized with Cy5 (*green*) (**a**, **b**), EphB3 visualized with Cy3 (*red*) (**a′**, **b′**) and merged images with nuclear staining by DAPI (*blue*) (**a″**, **b″**) in the MCL (**a**–**a″**) and parenchyma of the anterior lobe (**b**–**b″**) are shown. The images in (**a**–**b**”) were observed using a FLUOVIEW FV1000 confocal microscope. *AL* anterior lobe; *IL* intermediate lobe; *MCL* marginal cell layer. **c**–**d″** Double-immunohistochemistry for phalloidin and SOX2 using 4% PFA-fixed frozen sections of the pituitary gland on P60. Phalloidin visualized with Alexa Fluor 488 (*green*) (**c**, **d**), SOX2 visualized with Cy3 (*red*) and merged images without (**c′**, **d′**) and with (**c″**, **d″**) nuclear staining by DAPI (*blue*) in the MCL (**c**–**c″**) and the parenchyma of the anterior lobe (**d**–**d″**) are shown. *Dotted lines* outline the marginal cell layer in (**c**, **c″**). *Arrowheads* in (**d**, **d″**) indicate the parenchymal-niche. The images in (**c**–**d**”) were observed using a BZ-8000 epifluorescence microscope. *AL* anterior lobe; *IL* intermediate lobe; *MCL* marginal cell layer. *Bars* 10 μm

EphB3 signal remained limited to the apical cell membrane of cells in the MCL-niche, ephrin-B2 signals localized not only to the apical membrane of MCL cells but also to the basolateral membrane of cells in the MCL-zone (Fig. 6a–a″, arrows). The same result was observed in the parenchymal-niche of the anterior lobe (Fig. 6b–b″, arrows). Especially, these ephrin-B2 signals localized in the basolateral membrane of the cells in the multiple cell layers beneath the MCL were hardly observed in the adult pituitary.

In summary, we demonstrated that EphB3 *cis*-interacts with ephrin-B2 in the apical membrane of highly polarized cells in the stem/progenitor cell niches throughout life. However, ephrin-B2 is additionally located in the EphB3-negative basolateral membranes of the MCL-zone and periphery of the parenchymal-niche in the neonatal pituitary gland (P5), suggesting the ability to form *trans*-interactions with other Ephs in neighboring cells. These data prompted us to search for the Eph interacting in *trans* with ephrin-B2 and the cells expressing this Eph around the niches in the immature pituitary gland (P5).

Localization of EphB2-expressing corticotropes in the neonatal pituitary gland

To identify the Eph *trans*-interacting with ephrin-B2 in the neonatal pituitary niches, we first examined the cell types adjacent to both niches on P5 by triple-immunohistochemical staining for SOX2, E-cadherin and one of several differentiated cell markers (pituitary

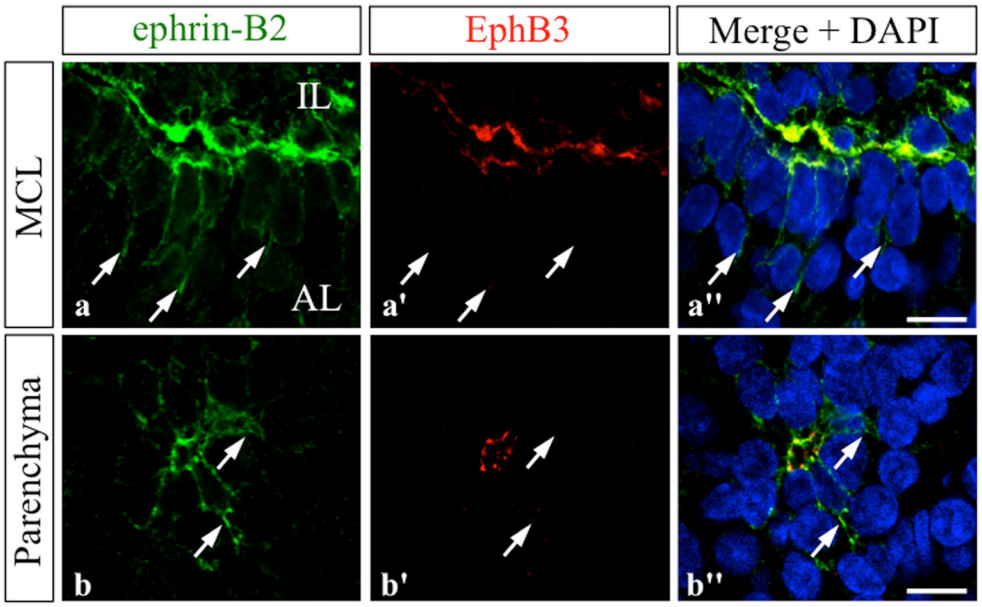

Fig. 6 Localization of ephrin-B2 and EphB3 in both niches of the neonatal pituitary gland. Immunohistochemistry for ephrin-B2 and EphB3 was performed using 95% ethyl alcohol-fixed cryosections of the pituitary gland on P5. Ephrin-B2 visualized with Cy5 (*green*) (**a**, **b**), EphB3 visualized with Cy3 (*red*) (**a′**, **b′**) and merged images with nuclear staining by DAPI (*blue*) (**a″**, **b″**) in the MCL (**a**–**a″**) and the parenchyma of the anterior lobe (**b**–**b″**) are shown. *Arrows* indicate the ephrin-B2 signal in the basolateral membrane of the cells in pituitary stem/progenitor cell niches. The images in (**a**–**b**″) were observed using a FLUOVIEW FV1000 confocal microscope. *AL* anterior lobe; *IL* intermediate lobe; *MCL* marginal cell layer. *Bars* 10 μm

hormones and isolectin-B4, which specifically binds to vascular endothelial cells) and counting the cell numbers immediately adjacent to each niche in the neonatal pituitary gland (Fig. 7). In the MCL-zone, GH-positive cells were the most common cells adjacent to E-cadherin-positive cells (48.3 ± 12.6 cells per 1 mm MCL), followed by ACTH-positive cells (14.1 ± 4.6), isolectin-B4-positive cells (6.9 ± 2.2), LHβ- and FSHβ-positive cells (6.8 ± 2.7) and PRL-positive cells (5.3 ± 3.1) (Fig. 7a–f, g), while TSHβ-positive cells were rarely found (1.2 ± 1.2) (Fig. 7d, g). In the parenchymal-niche of the anterior lobe, cells adjacent to SOX2- and E-cadherin-double positive cells were most often GH-positive cells (2.7 ± 0.4 cells per parenchymal-niche) or ACTH-positive cells (2.1 ± 0.6), rather than PRL-positive cells (0.4 ± 0.3), TSHβ-positive cells (0.5 ± 0.19), LHβ- and FSHβ-positive cells (0.2 ± 0.1), or isolectin-B4-positive cells (0.3 ± 0.1) (Fig. 7a′–f′, g′). These results demonstrate that GH- and ACTH-positive cells tend to attach to both niches on P5. Although none of the candidate Eph partners for ephrin-B2 were detected in GH-producing cells, EphB2 specifically localized to ACTH-producing corticotropes (Fig. 2). We therefore performed double-immunohistochemistry for ephrin-B2 and EphB2 on P5 (Fig. 8). Results demonstrated that EphB2-positive corticotropes were in contact with ephrin-B2-single positive stem/progenitor cells beneath the MCL on P5 (Fig. 8, arrowheads). These data indicate that EphB2 produced by corticotropes *trans*-interacts with ephrin-B2.

Discussion

We previously reported that ephrin-B2 exists in SOX2/CAR double-positive stem/progenitor cells in both the MCL- and parenchymal-niches in the rat pituitary gland and may play a role in regulating the maintenance of stem/progenitor cells and *trans*-differentiation into committed cells (Yoshida et al. 2015). In this study, we aimed to identify Ephs interacting with ephrin-B2 and the cells that express these proteins in the rat pituitary gland. Consequently, we demonstrated that each candidate interacting partner for ephrin-B2 exhibits cell type-specific localization and that EphB3 and EphB2 interact with ephrin-B2 in *cis* and in *trans*, respectively.

Although Eph localization has been reported in several tissues such as the intestine, brain, skin and pancreas (Batlle et al. 2002; Genander et al. 2010; Konstantinova et al. 2007; Nomura et al. 2010), it has not previously been investigated in the pituitary gland. In the present study, our observations demonstrate that each candidate ephrin-B2 interacting partner (EphA4, EphB1, EphB2, EphB3 and EphB4) is expressed in a cell type-specific manner in the pituitary gland. First, we confirmed that *EphA4* is localized in nucleated cells of the posterior lobe, where ephrin-B2 is absent, suggesting that EphA4 in the posterior lobe interacts with A-class ephrins. In fact, expression of ephrin-A5, a ligand for EphA4, has been reported in the posterior lobe (Zarbalis and Wurst 2000). In the anterior lobe, which is composed of five types of endocrine cells as well as non-

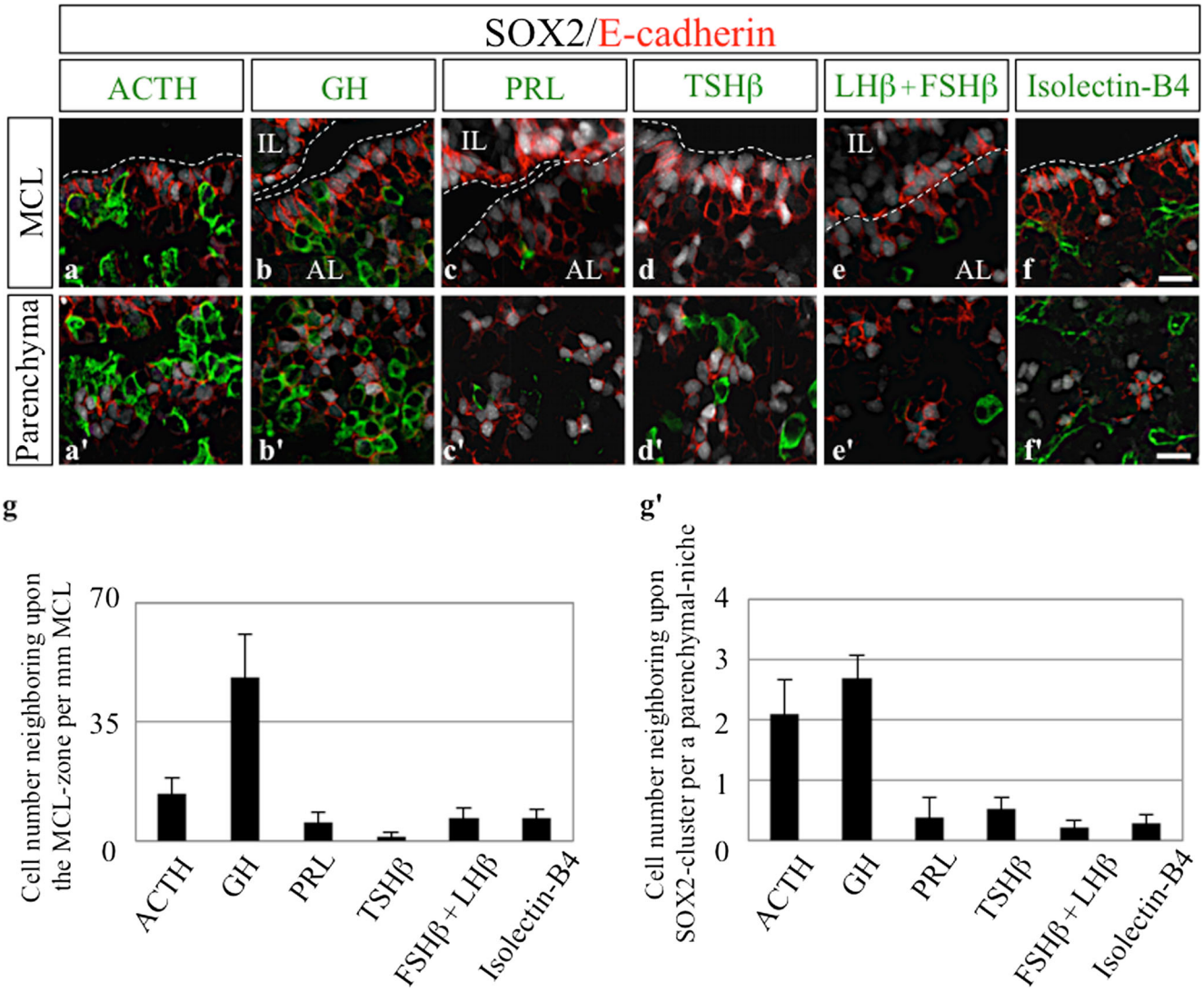

Fig. 7 Identification and quantification of contiguous cells of each niche in the neonatal pituitary gland. Immunohistochemistry for SOX2, E-cadherin and differentiated cell markers was performed using 4% PFA-fixed frozen sections of the pituitary gland on P5. Merged images of SOX2 visualized with Cy5 (*white*), E-cadherin visualized with Cy3 (*red*) and differentiated cell markers (**a**, **a′** ACTH, **b**, **b′** GH, **c**, **c′** PRL, **d**, **d′** TSHβ, **e**, **e′** LHβ/FSHβ and **f**, **f′** isolectin-B4) visualized with FITC (*green*) in the MCL-niche (**a**–**f**) and the parenchymal-niche (**a′**–**f′**) of the anterior lobe are shown. *Dotted lines* outline the marginal cell layer. All images were observed using a BZ-8000 epifluorescence microscope. *AL* anterior lobe; *IL* intermediate lobe; *MCL* marginal cell layer. *Bars* 20 μm. **g**, **g′** Counts of neighboring cells in both niches on P5. Each bar shows the number of cells neighboring E-cadherin-positive cells under the MCL zone (**g**) and neighboring SOX2/E-cadherin-double positive cells in the parenchymal-niche of the anterior lobe (**g′**). Data are presented as the number of cells per 1 mm (**g**) and the number of cells per parenchymal-niche (**g′**). Data are presented as means ± SD for three animals

endocrine cells, EphB1, EphB2, EphB3 and EphB4 were found specifically in gonadotropes, corticotropes, stem/progenitor cells and endothelial cells, respectively. Cell type-specific localizations of Ephs have been reported in various other tissues. Wang et al. reported that *EphB4* is expressed in endothelial cells in veins but not arteries (Wang et al. 1998) and mice deficient in *EphB4* show early embryonic lethality with disturbed arterio-venous differentiation (Gerety et al. 1999). In addition, the present data showed that EphB1 and EphB2 localize at least to the cytoplasm. In the pancreatic islets, Konstantinova et al. reported that EphA5 and ephrin-A5 are mainly localized in the insulin secretory granules in the cytoplasm and plasma membrane of β-cells, respectively and regulate both basal and glucose-stimulated hormone secretion in mouse and human (Konstantinova et al. 2007). Taken together, EphBs located in the cytoplasm may be involved in hormone secretions in the pituitary gland. In addition, ephrin/Eph signaling is known to regulate boundary formation during development of several tissues (Batlle et al. 2002; Mellitzer et al. 1999). Taken together with our results of cell type-specific localization of EphBs in the anterior lobe of the pituitary, ephrin-Bs/

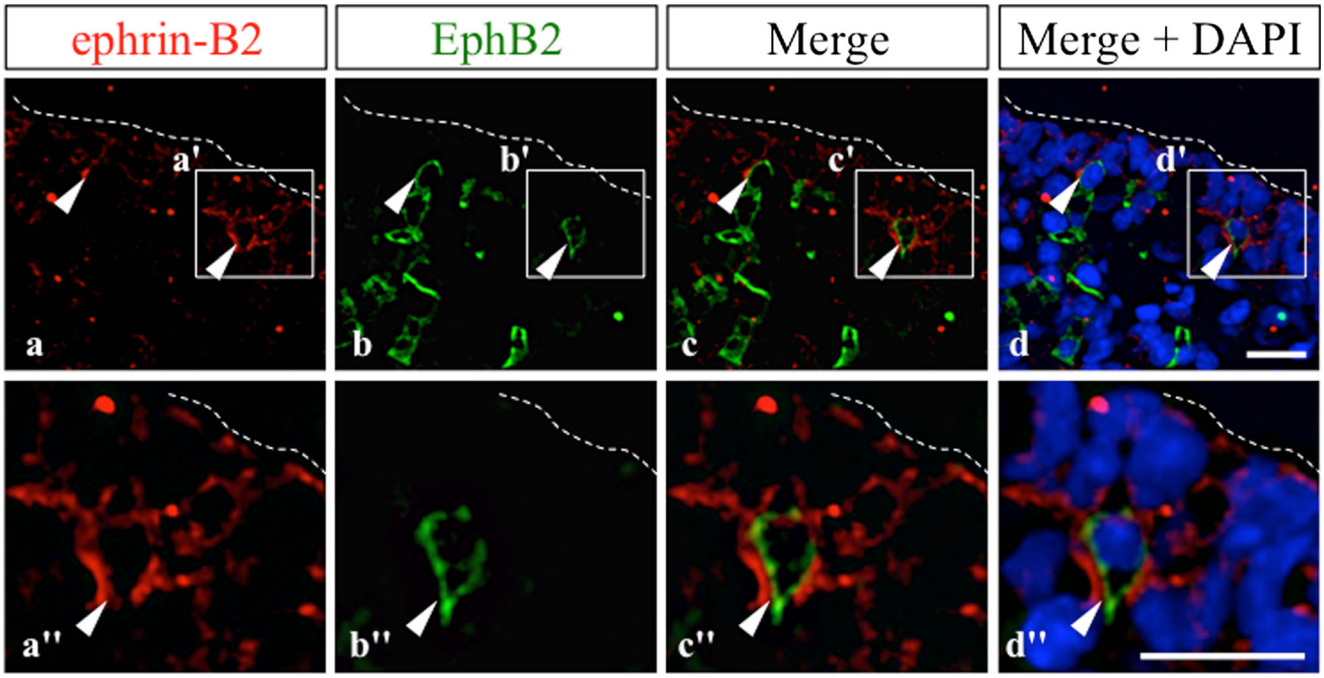

Fig. 8 Localization of ephrin-B2 and EphB2 in the neonatal pituitary. Double-immunohistochemistry for ephrin-B2 and EphB2 was performed using 4% PFA-fixed frozen sections of the pituitary gland on P5. Ephrin-B2 visualized with Cy3 (*red*) (**a**), EphB2 visualized with Cy5 (*green*) (**b**) and merged images without (**c**) and with (**d**) nuclear staining by DAPI (*blue*) are shown. The *boxed areas* in (**a′**–**d′**) are enlarged in (**a″**–**d″**). *Arrowheads* indicate basolateral ephrin-B2 signal in cells neighboring EphB2-positive cells. *Dotted lines* outline the marginal cell layer in the anterior lobe. All images were observed using a BZ-8000 epifluorescence microscope. *Bars* 20 μm

EphBs signaling might be involved in the distribution of respective endocrine cells in the developing pituitary.

Next, we identified EphB2 and EphB3 as potential interacting partners for ephrin-B2 in the pituitary gland. EphB3 co-localizes with ephrin-B2 in the apical membrane of stem/progenitor cells in both pituitary niches, indicating that they form a *cis*-interaction to generate parallel or anti-parallel signaling (Kania and Klein 2016). In contrast, in the neonatal pituitary gland, EphB2-producing corticotropes are in contact with ephrin-B2-positive stem/progenitor cells in the MCL-zone, suggesting that they form a *trans*-interaction to create bi-directional signaling. In the adult pituitary gland, Andoniadou et al. performed *Sox2*-lineage tracing analysis and found that most SOX2-positive cells are in a quiescent state in both niches under normal physiological conditions (Andoniadou et al. 2013). In contrast, SOX2-positive cells in the neonatal pituitary gland have a greater potential to proliferate and differentiate than those in the adult pituitary gland (Davis et al. 2010; Gremeaux et al. 2012; Vankelecom and Chen 2014; Ward et al. 2006; Zhu et al. 2007). Moreover, immunohistochemical observations suggest that stem/progenitor cells migrate from the MCL and form the MCL-zone during the postnatal pituitary growth wave (Chen et al. 2013; Gremeaux et al. 2012). The present study did not investigate the function of ephrin-B2 and EphB2-mediated reverse and forward signaling in stem/progenitor cells and corticotropes. However, there are reports that *trans*-interactions between ephrin-B2 and EphB proteins promote cell repulsion and migration in several cell lines, including gliomas (Nakada et al. 2010), melanomas (Meyer et al. 2005) and intestinal epithelia (Hafner et al. 2005). Taken together, these findings suggest that activation of ephrin-B2 signaling in pituitary stem/progenitor cells may be involved in the acceleration of cell migration from niches in the early postnatal period, though this hypothesis remains to be tested.

Another point to note is that EphB3 exists ubiquitously in the apical cell membranes of both pituitary niches throughout life. Several membrane proteins, such as E-cadherin (Fauquier et al. 2008), GFRα2 (Garcia-Lavandeira et al. 2009), CAR (Chen et al. 2013) and ephrin-B2 (Yoshida et al. 2015) are also known to localize to the pituitary niches. Among these, only EphB3 shows specific and ubiquitous localization in the apical cell membranes of both pituitary niches. It has been demonstrated that apical constriction in the neural tube closure and gastrulation are important for embryonic development (Martin and Goldstein 2014; Sawyer et al. 2010). In the adult neural stem cell niche, apically polarized cell populations are observed as rosette structures in the brain (Harding et al. 2014; Mirzadeh et al. 2008) and such apical polarizations are required for asymmetric division of neural stem cells (Kosodo et al. 2004). Interestingly, a complex consisting of Eph and FAK (focal adhesion kinase) is necessary for cytoskeletal organization and apical constriction in *Strongylocentrotus purpuratus* (Krupke and Burke 2014) and EphB3 and

EphB2 regulate the development of apical constriction in the mouse pancreas (Villasenor et al. 2010). In addition to interacting with ephrin-B proteins, EphB3 contains a PSD-95, Dlg, ZO-1 (PDZ)-binding domain and is therefore able to interact with proteins containing PDZ domains, such as the tight junction-associated protein AF6 (Buchert et al. 1999). Thus, the apical localization of EphB3 in the pituitary gland may be involved in polarization and maintenance of the architecture of pituitary niches.

In summary, we demonstrated that the juxtacrine factor ephrin-B2, which is expressed in pituitary stem/progenitor cells, has two interacting partners; EphB3 inside pituitary niches and EphB2 outside of these niches. In particular, the *cis*-interaction with EphB3 in the pituitary stem/progenitor cell niches is a novel mechanism for regulating pituitary stem cell niches and may be involved in sustaining the architecture of these niches.

Acknowledgements The authors wish to thank Dr. A.F. Parlow and the NIDDK for antibodies against pituitary hormones, Dr. S. Tanaka at Shizuoka University for antibodies against human ACTH and GH and K. Kawai for his excellent technical assistance. This work was partially supported by JSPS KAKENHI (grant numbers 21380184 to YK, 24580435 to TK and 16 K18818 to SY); the MEXT-Supported Program for the Strategic Research Foundation at Private Universities; a research grant (A) to YK from the Institute of Science and Technology, Meiji University; and the Meiji University International Institute for BioResource Research (MUIIR).

References

Akada M, Harada K, Negishi M, Katoh H (2014) EphB6 promotes anoikis by modulating EphA2 signaling. Cell Signal 26:2879–2884

Andoniadou CL, Matsushima D, Mousavy Gharavy SN, Signore M, Mackintosh AI, Schaeffer M, Gaston-Massuet C, Mollard P, Jacques TS, Le Tissier P, Dattani MT, Pevny LH, Martinez-Barbera JP (2013) Sox2(+) stem/progenitor cells in the adult mouse pituitary support organ homeostasis and have tumor-inducing potential. Cell Stem Cell 13:433–445

Anselmo A, Lauranzano E, Soldani C, Ploia C, Angioni R, D'Amico G, Sarukhan A, Mazzon C, Viola A (2016) Identification of a novel agrin-dependent pathway in cell signaling and adhesion within the erythroid niche. Cell Death Differ 23:1322–1330

Arvanitis D, Davy A (2008) Eph/ephrin signaling: networks. Genes Dev 22:416–429

Ashton RS, Conway A, Pangarkar C, Bergen J, Lim KI, Shah P, Bissell M, Schaffer DV (2012) Astrocytes regulate adult hippocampal neurogenesis through ephrin-B signaling. Nat Neurosci 15:1399–1406

Batlle E, Henderson JT, Beghtel H, van den Born MM, Sancho E, Huls G, Meeldijk J, Robertson J, van de Wetering M, Pawson T, Clevers H (2002) Beta-catenin and TCF mediate cell positioning in the intestinal epithelium by controlling the expression of EphB/ephrinB. Cell 111:251–263

Buchert M, Schneider S, Meskenaite V, Adams MT, Canaani E, Baechi T, Moelling K, Hovens CM (1999) The junction-associated protein AF-6 interacts and clusters with specific Eph receptor tyrosine kinases at specialized sites of cell-cell contact in the brain. J Cell Biol 144:361–371

Chen CC, Chuong CM (2012) Multi-layered environmental regulation on the homeostasis of stem cells: the saga of hair growth and alopecia. J Dermatol Sci 66:3–11

Chen J, Gremeaux L, Fu Q, Liekens D, Van Laere S, Vankelecom H (2009) Pituitary progenitor cells tracked down by side population dissection. Stem Cells 27:1182–1195

Chen M, Kato T, Higuchi M, Yoshida S, Yako H, Kanno N, Kato Y (2013) Coxsackievirus and adenovirus receptor-positive cells compose the putative stem/progenitor cell niches in the marginal cell layer and parenchyma of the rat anterior pituitary. Cell Tissue Res 354:823–836

Davis SW, Castinetti F, Carvalho LR, Ellsworth BS, Potok MA, Lyons RH, Brinkmeier ML, Raetzman LT, Carninci P, Mortensen AH, Hayashizaki Y, Arnhold IJ, Mendonca BB, Brue T, Camper SA (2010) Molecular mechanisms of pituitary organogenesis: in search of novel regulatory genes. Mol Cell Endocrinol 323:4–19

Egea J, Klein R (2007) Bidirectional Eph-ephrin signaling during axon guidance. Trends Cell Biol 17:230–238

Fauquier T, Rizzoti K, Dattani M, Lovell-Badge R, Robinson IC (2008) SOX2-expressing progenitor cells generate all of the major cell types in the adult mouse pituitary gland. Proc Natl Acad Sci U S A 105:2907–2912

Freywald A, Sharfe N, Roifman CM (2002) The kinase-null EphB6 receptor undergoes transphosphorylation in a complex with EphB1. J Biol Chem 277:3823–3828

Fu Q, Vankelecom H (2012) Regenerative capacity of the adult pituitary: multiple mechanisms of lactotroph restoration after transgenic ablation. Stem Cells Dev 21:3245–3257

Fu Q, Gremeaux L, Luque RM, Liekens D, Chen J, Buch T, Waisman A, Kineman R, Vankelecom H (2012) The adult pituitary shows stem/progenitor cell activation in response to injury and is capable of regeneration. Endocrinology 153:3224–3235

Fujiwara K, Davaadash B, Kikuchi M, Takigami S, Yashiro T (2008) Estrogen suppresses retinaldehyde dehydrogenase 1 expression in the anterior pituitary glands of female rats. Endocr J 55:91–96

Garcia-Lavandeira M, Quereda V, Flores I, Saez C, Diaz-Rodriguez E, Japon MA, Ryan AK, Blasco MA, Dieguez C, Malumbres M, Alvarez CV (2009) A GRFa2/Prop1/stem (GPS) cell niche in the pituitary. PLoS ONE 4:e4815

Genander M, Holmberg J, Frisen J (2010) Ephrins negatively regulate cell proliferation in the epidermis and hair follicle. Stem Cells 28:1196–1205

Gerety SS, Wang HU, Chen ZF, Anderson DJ (1999) Symmetrical mutant phenotypes of the receptor EphB4 and its specific transmembrane ligand ephrin-B2 in cardiovascular development. Mol Cell 4:403–414

Gremeaux L, Fu Q, Chen J, Vankelecom H (2012) Activated phenotype of the pituitary stem/progenitor cell compartment during the early-postnatal maturation phase of the gland. Stem Cells Dev 21:801–813

Gurniak CB, Berg LJ (1996) A new member of the Eph family of receptors that lacks protein tyrosine kinase activity. Oncogene 13:777–786

Hafner C, Meyer S, Hagen I, Becker B, Roesch A, Landthaler M, Vogt T (2005) Ephrin-B reverse signaling induces expression of wound healing associated genes in IEC-6 intestinal epithelial cells. World J Gastroenterol 11:4511–4518

Harding MJ, McGraw HF, Nechiporuk A (2014) The roles and regulation of multicellular rosette structures during morphogenesis. Development 141:2549–2558

Higuchi M, Yoshida S, Ueharu H, Chen M, Kato T, Kato Y (2015) PRRX1- and PRRX2-positive mesenchymal stem/progenitor cells are involved in vasculogenesis during rat embryonic pituitary development. Cell Tissue Res 361:557–565

Ishii M, Nakajima T, Ogawa K (2011) Complementary expression of EphB receptors and ephrin-B ligand in the pyloric and duodenal epithelium of adult mice. Histochem Cell Biol 136:345–356

Jensen PL (2000) Eph receptors and ephrins. Stem Cells 18:63–64

Kania A, Klein R (2016) Mechanisms of ephrin-Eph signalling in development, physiology and disease. Nat Rev Mol Cell Biol 17:240–256

Kato H, Kuwako K, Suzuki M, Tanaka S (2004) Gene expression patterns of pro-opiomelanocortin-processing enzymes PC1 and PC2 during postnatal development of rat corticotrophs. J Histochem Cytochem 52:943–957

Kikuchi M, Yatabe M, Kouki T, Fujiwara K, Takigami S, Sakamoto A, Yashiro T (2007) Changes in E- and N-cadherin expression in developing rat adenohypophysis. Anat Rec (Hoboken) 290:486–490

Konstantinova I, Nikolova G, Ohara-Imaizumi M, Meda P, Kucera T, Zarbalis K, Wurst W, Nagamatsu S, Lammert E (2007) EphA-Ephrin-A-mediated beta cell communication regulates insulin secretion from pancreatic islets. Cell 129:359–370

Kosodo Y, Roper K, Haubensak W, Marzesco AM, Corbeil D, Huttner WB (2004) Asymmetric distribution of the apical plasma membrane during neurogenic divisions of mammalian neuroepithelial cells. EMBO J 23:2314–2324

Krupke OA, Burke RD (2014) Eph-Ephrin signaling and focal adhesion kinase regulate actomyosin-dependent apical constriction of ciliary band cells. Development 141:1075–1084

Li YC, Bai WZ, Hashikawa T (2007) Regionally varying F-actin network in the apical cytoplasm of ependymocytes. Neurosci Res 57:522–530

Martin AC, Goldstein B (2014) Apical constriction: themes and variations on a cellular mechanism driving morphogenesis. Development 141:1987–1998

Mellitzer G, Xu Q, Wilkinson DG (1999) Eph receptors and ephrins restrict cell intermingling and communication. Nature 400:77–81

Meyer S, Hafner C, Guba M, Flegel S, Geissler EK, Becker B, Koehl GE, Orso E, Landthaler M, Vogt T (2005) Ephrin-B2 overexpression enhances integrin-mediated ECM-attachment and migration of B16 melanoma cells. Int J Oncol 27:1197–1206

Mirzadeh Z, Merkle FT, Soriano-Navarro M, Garcia-Verdugo JM, Alvarez-Buylla A (2008) Neural stem cells confer unique pinwheel architecture to the ventricular surface in neurogenic regions of the adult brain. Cell Stem Cell 3:265–278

Munthe E, Rian E, Holien T, Rasmussen A, Levy FO, Aasheim H (2000) Ephrin-B2 is a candidate ligand for the Eph receptor, EphB6. FEBS Lett 466:169–174

Murai KK, Pasquale EB (2003) 'Eph'ective signaling: forward, reverse and crosstalk. J Cell Sci 116:2823–2832

Nakada M, Anderson EM, Demuth T, Nakada S, Reavie LB, Drake KL, Hoelzinger DB, Berens ME (2010) The phosphorylation of ephrin-B2 ligand promotes glioma cell migration and invasion. Int J Cancer 126:1155–1165

Nomura T, Goritz C, Catchpole T, Henkemeyer M, Frisen J (2010) EphB signaling controls lineage plasticity of adult neural stem cell niche cells. Cell Stem Cell 7:730–473

Pasquale EB (2005) Eph receptor signalling casts a wide net on cell behaviour. Nat Rev Mol Cell Biol 6:462–475

Rizzoti K, Akiyama H, Lovell-Badge R (2013) Mobilized adult pituitary stem cells contribute to endocrine regeneration in response to physiological demand. Cell Stem Cell 13:419–432

Sawyer JM, Harrell JR, Shemer G, Sullivan-Brown J, Roh-Johnson M, Goldstein B (2010) Apical constriction: a cell shape change that can drive morphogenesis. Dev Biol 341:5–19

Tanaka S, Kurosumi K (1992) A certain step of proteolytic processing of proopiomelanocortin occurs during the transition between two distinct stages of secretory granule maturation in rat anterior pituitary corticotrophs. Endocrinology 131:779–786

Truitt L, Freywald T, DeCoteau J, Sharfe N, Freywald A (2010) The EphB6 receptor co-operates with c-Cbl to regulate the behaviour of breast cancer cells, Cancer Res 70:1141-1153

Vankelecom H, Chen J (2014) Pituitary stem cells: where do we stand? Mol Cell Endocrinol 385:2–17

Villasenor A, Chong DC, Henkemeyer M, Cleaver O (2010) Epithelial dynamics of pancreatic branching morphogenesis. Development 137:4295–4305

Wang HU, Chen ZF, Anderson DJ (1998) Molecular distinction and angiogenic interaction between embryonic arteries and veins revealed by ephrin-B2 and its receptor Eph-B4. Cell 93:741–753

Ward RD, Raetzman LT, Suh H, Stone BM, Nasonkin IO, Camper SA (2005) Role of PROP1 in pituitary gland growth. Mol Endocrinol 19:698–710

Ward RD, Stone BM, Raetzman LT, Camper SA (2006) Cell proliferation and vascularization in mouse models of pituitary hormone deficiency. Mol Endocrinol 20:1378–1390

Willems C, Fu Q, Roose H, Mertens F, Cox B, Chen J, Vankelecom H (2016) Regeneration in the pituitary after cell-ablation injury: time-related aspects and molecular analysis. Endocrinology 157:705–721

Wollesen T, Loesel R, Wanninger A (2009) Pygmy squids and giant brains: mapping the complex cephalopod CNS by phalloidin staining of vibratome sections and whole-mount preparations. J Neurosci Methods 179:63–67

Yoshida S, Kato T, Higuchi M, Chen M, Ueharu H, Nishimura N, Kato Y (2015) Localization of juxtacrine factor ephrin-B2 in pituitary stem/progenitor cell niches throughout life. Cell Tissue Res 359:755–766

Yoshida S, Kato T, Kato Y (2016a) Regulatory system for stem/progenitor cell niches in the adult rodent pituitary. Int J Mol Sci 17:75

Yoshida S, Nishimura N, Ueharu H, Kanno N, Higuchi M, Horiguchi K, Kato T, Kato Y (2016b) Isolation of adult pituitary stem/progenitor cell clusters located in the parenchyma of the rat anterior lobe. Stem Cell Res 17:318–329

Zaglia T, Di Bona A, Chioato T, Basso C, Ausoni S, Mongillo M (2016) Optimized protocol for immunostaining of experimental GFP-expressing and human hearts. Histochem Cell Biol 146:407–419

Zarbalis K, Wurst W (2000) Expression domains of murine ephrin-A5 in the pituitary and hypothalamus. Mech Dev 93:165–168

Zhu X, Gleiberman AS, Rosenfeld MG (2007) Molecular physiology of pituitary development: signaling and transcriptional networks. Physiol Rev 87:933–963